



Comparative study of naproxen degradation in water by UV/persulfate and UV/H₂O₂ processes

Yu-qiong Gao^{a,*}, Nai-yun Gao^b, Da-qiang Yin^b, Ju-xiang Chen^c

^aSchool of Environment and Architecture, University of Shanghai for Science and Technology, Shanghai 200093, China, Tel. +86 21 55275979, email: gaoyq@usst.edu.cn

^bState Key Laboratory of Pollution Control and Resource Reuse, Key Laboratory of Yangtze River Water Environment, Ministry of Education, College of Environmental Science and Engineering, Tongji University, Shanghai 200092, China, Tel. +86 21 55275979, emails: gaonaiyun2016@163.com (N.Y. Gao), yindaqiang2016@163.com (D.Q. Yin)

^cCollege of Architecture and Civil Engineering, Xinjiang University, Urumqi 830047, China, Tel. +86 21 55275979, email:1455087064@qq.com

Received 3 February 2017; Accepted 16 May 2017

ABSTRACT

This study comparatively investigated naproxen (NPX) degradation by UV/persulfate (UV/PS) and UV/H₂O₂ processes under different conditions. Direct UV photolysis of NPX was limited. The degradation rate of NPX was largely enhanced by UV/PS and UV/H₂O₂ processes due to high-reactive radicals (SO₄^{•-} or/and •OH) formed. The second-order rate constants of NPX with SO₄^{•-} and •OH were determined as 7.81 × 10⁹ and 6.22 × 10¹⁰ M⁻¹ s⁻¹, respectively. The pseudo-first-order rate constant (*k*) of NPX increases linearly with the initial concentration of PS in UV/PS process, whereas the *k* in the UV/H₂O₂ process contains the best dosage of H₂O₂. Acidic conditions were found to be favorable for NPX removal in UV/PS process, while the maximum NPX removal was observed at pH 6 in UV/H₂O₂ process. Further, the Cl⁻ promotes NPX degradation in both of the processes, and the effect of HCO₃⁻ on degradation of the NPX was opposite in two processes. Humic acid shows a higher inhibition in UV/H₂O₂ process in comparison with that in UV/PS process. The lower mineralization efficiency indicates that the products of NPX were more reluctant to the two systems compared with its parent drug. These results indicated that both processes are potential alternatives to control water pollution contaminated by drugs such as NPX.

Keywords: Naproxen; UV; Sulfate radicals; Hydroxyl radicals; Degradation; Kinetics

1. Introduction

Naproxen (NPX), a non-steroidal anti-inflammatory drug (NSAIDs), is mostly used in medical care as an analgesic, antiarthritic and antirheumatic [1]. Like other drug products, NPX can enter into the sewer system through urine and faeces that are discharged into wastewater treatment plants. Unfortunately, our conventional water/wastewater treatment processes are not specifically focused on removing these drugs. Therefore, these drugs may remain in the

effluents after the treatment [2]. In the recent past, NPX has been detected in a variety of environmental water at concentrations ranging between ng L⁻¹ and µg L⁻¹ [3,4]. Similar to the other NSAIDs, its presence may bring about a potential harmful effect on human health and ecosystems [5,6]. It has been reported that people who ingest trace amounts of NPX for a long time may develop a risk of having heart attacks or strokes as compared with those other people who are not exposed to the NPX drug [7]. There is need to pay more attention on the development of effective remediation technology for removal of NPX in the aquatic environment, so that its risks and prospective adverse effects on people are reduced.

* Corresponding author.

Advance oxidation processes (AOPs) have attracted considerable attention for their effective destruction and mineralization of organic contaminants. Among a range of AOPs, UV-based oxidation process has a higher potential due to its high treatment efficiency and low cost [8]. Generally, organic contaminants can be degraded through direct photolysis in aquatic environment, where its degradation efficiency will mostly depend on the compound's capacity to absorb photons of the incident light [9]. In as much as UV irradiation is capable of destructing organic compounds, under UV-254 nm irradiation, the addition of H₂O₂ can also greatly improve the degradation efficiency through the formation of hydroxyl radicals (•OH) (Eq. (1)). This is because it has a high redox potential of 2.8 V [10], and can, therefore, easily and non-selectively oxidize a large variety of organic contaminants. Recently, another oxidant, persulfate (PS), has attracted attention of researchers and scholars because of its longer half-life in the subsurface water/soil as compared with that of H₂O₂. As different from H₂O₂, PS has several advantages, including easy storage and transport due to its moderate stability in the ambient temperature, high water solubility as well as low cost [11]. Even though PS is stable under normal conditions, sulfate radical (SO₄•⁻) can, however, be generated by UV irradiation [12] (Eq. (2)), as well as other activation methods, like heat [13] and transition metals [14]. SO₄•⁻ has a high redox potential of 2.6 V, which is close to that of •OH, and it exhibits an excellent removal efficiency towards most of organic pollutants in water [12–14].



The aim of this study is to comparatively investigate NPX by UV/PS and UV/H₂O₂ processes. Quantum yield of NPX by UV irradiation was calculated. Second-order rate constants of NPX with SO₄•⁻ and •OH were also determined by competition kinetics experiment. The key factors, namely oxidant concentration, pH, anions and humic acid (HA), on the NPX degradation efficiency by UV/PS and UV/H₂O₂ processes were compared. We also evaluated the two processes used in removal of NPX in natural water. Finally, the mineralization of NPX by the two processes was assessed.

2. Materials and methods

2.1. Chemicals

NPX was purchased from Sigma-Aldrich (St Louis, Missouri, USA) and the selected physicochemical properties were listed in Table 1 [15]. High-performance liquid

chromatography (HPLC)-grade acetonitrile, used as the mobile phase, was also obtained from Sigma-Aldrich. Then, atrazine, sodium persulfate, hydrogen peroxide (H₂O₂, 30%), methanol (MeOH) and tert-butanol (TBA) had been acquired from Shanghai Jingchun Industry Co., Ltd. (Shanghai, China). Ultrapure water produced from a Millipore water purification system (18.2 MΩ cm, Billerica, MA, USA) was used in the preparation of the solutions.

2.2. Experimental procedures

UV/PS and UV/H₂O₂ tests were performed in a collimated beam apparatus equipped with a low-pressure UV–mercury lamp [16]. The average UV fluence rate value of the lamp was about $4.46 \times 10^{-8} \text{ E L}^{-1} \text{ s}^{-1}$, measured through the atrazine actinometer method [8], and the correspondence of UV intensity was 261 μW cm⁻². The optical path length of the reactor was determined to be 12.4 cm by using H₂O₂ as an actinometer [17]. A minimum of 30 min warm-up time ascertained a stabilized UV emission output. In the treatment process, a reactor containing 20 μM NPX solution was put under the lampshade. Oxidant stock solution (PS or H₂O₂) was freshly prepared immediately before use. Appropriate volumes of oxidant stock solutions were pre-added into the NPX solution. A gentle stirring made sure that the solution was completely mixed. The oxidation was initiated once the Petri dishes were moved under the UV lamps. The solution pH was adjusted by 10 mM phosphate buffer. At the predetermined time intervals, 0.8 mL solution was sampled and quenched by 0.2 mL methanol that was pre-filled in sample bottles before HPLC analysis. All the experiments were conducted in duplicate. The mean values were recorded and reported.

2.3. Analytical methods

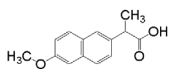
NPX and atrazine were analyzed using a HPLC (Waters e2695, USA) equipped with a Symmetry C18 column (4.6 mm × 250 mm, 5 μm, Waters, USA) by a UV detector wavelength of 230 and 223 nm, respectively. The value of limit of quantitation (LOQ, S/N = 10) for NPX was 5.6 μg L⁻¹. The mobile phase for NPX consisted of 70%/30% (v/v) acetonitrile and 0.1% formic acid in Milli-Q water at a flow rate of 0.8 mL min⁻¹. The mobile phase for atrazine consisted of 60%/40% acetonitrile and Milli-Q water at a flow rate of 0.8 mL min⁻¹. The sample injection volume was 10 μL. Total organic carbon (TOC) was measured by a TOC analyzer (Shimadzu TOC 5050A) with autosampler ASI5000. The PS concentration was determined spectrophotometrically with the iodometric titration method modified by Liang et al. [18], and the concentration of H₂O₂ was determined spectrophotometrically by use of the titanium oxalate method [19].

3. Results and discussion

3.1. Degradation of NPX by UV, UV/PS and UV/H₂O₂

First, we examined the direct UV photolysis of NPX as illustrated in Fig. 1(b). UV photolysis of NPX followed a pseudo-first-order reaction with the rate constant (*k*) of 0.00238 min⁻¹, indicating that only 13.0% of NPX could be removed under 1 h UV irradiation alone. In UV direct

Table 1
Selected physicochemical properties of NPX

Chemical formula	Chemical structure	Molar mass (g mol ⁻¹)	Log <i>K</i> _{ow}	pKa
C ₁₄ H ₁₄ O ₃		230.26	3.18	4.45

photolysis, the removal efficiency of the contaminant largely depends on two key parameters; molar coefficient and quantum yield [20]. For this study, the molar adsorption coefficient (ϵ_{254} M⁻¹ cm⁻¹) of NPX was measured as 4,818 M⁻¹ cm⁻¹ (pH 7). According to Eq. (3), the quantum yield (Φ_{254} , mol E⁻¹) of NPX can be calculated as 0.0065 mol E⁻¹ [21], which corresponds with the results of Pereira et al. [22] (0.0093 ± 0.0027). Therefore, the relatively low quantum yield of NPX can explain the low efficiency of NPX by direct UV photolysis.

$$\ln \frac{c_t}{c_0} = -2.303I_0\Phi\epsilon t = -2.303q\Phi\epsilon t = -k_{app}t \quad (3)$$

where c_t is the concentration of NPX (mol L⁻¹) at time t , c_0 is the initial concentration of NPX (mol L⁻¹), k_{app} is the pseudo-first-order rate constant (min⁻¹), I_0 is the average photonic intensity per volume (E L⁻¹ s⁻¹), L is the reactor

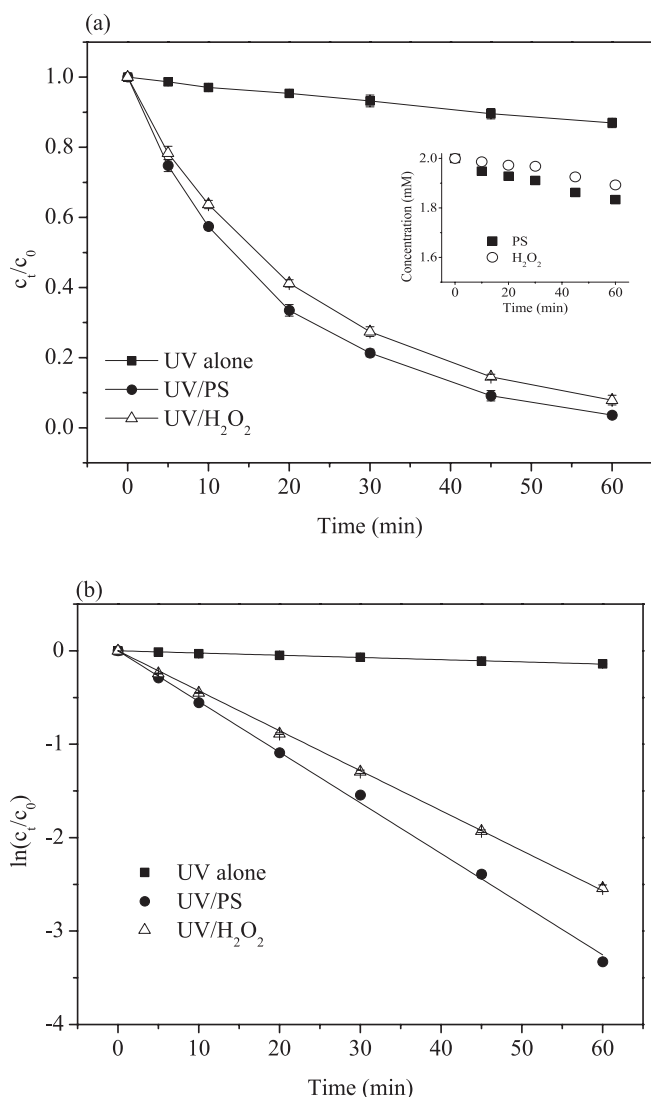


Fig. 1. (a) Degradation of NPX by UV, UV/PS and UV/H₂O₂. (b) Linear plots of NPX degradation in the different systems. Conditions: [NPX]₀ = 20 μM, [PS]₀ = [H₂O₂]₀ = 2 mM, pH = 7.

optical light path (cm), q is the photon flux (E s⁻¹ cm⁻²), ϵ is the molar extinction coefficient of organic material for UV (L mol⁻¹ cm⁻¹) and Φ is the quantum yield of photodegradation for UV (mol E⁻¹).

The degradation of NPX by UV/PS and UV/H₂O₂ processes was compared with direct UV photolysis (as shown in Fig. 1). In the control experiment, there was no change of NPX concentration in the presence of 2 mM oxidant ([Oxidant]₀/[NPX]₀ = 100) without UV irradiation. We can notice that the degradation of NPX in UV/PS and UV/H₂O₂ processes also followed the pseudo-first-order kinetics. The addition of PS and H₂O₂ obviously increased the degradation rates from 0.00238 to 0.0542 and 0.0428 min⁻¹, respectively, due to the generation of highly reactive SO₄^{•-} and •OH (Eqs. (1) and (2)). Furthermore, the degradation rate of NPX in the UV/PS system was higher than that in the UV/H₂O₂ system under the same amount of oxidant. To approximate the costs involved in practice, an economic comparison of three systems was conducted by determining the electrical energy per order (EE/O) (Eq. (4)) [23]:

$$EE/O = \frac{Pt}{V} \quad (4)$$

where P is the electrical power (kW), t is the irradiation time (h) and V is the volume of treated solution (m³). The EE/O and cost by three different systems are summarized in Table 2. As observed in Table 2, we realized that UV/PS was the most economical system among three systems.

3.2. Rate constants of NPX with SO₄^{•-} and •OH

Considering the direct photolysis of NPX at 254 nm, the second-order rate constants of NPX with SO₄^{•-} and •OH were determined by competition kinetics, according to Eq. (5) [9]. Atrazine (ATR) was chosen as the reference for the rate constants determination. The second-order rate constants of SO₄^{•-} and •OH with ATR were found to be 1.4×10^9 and 1.8×10^{10} M⁻¹ s⁻¹, respectively [24,25].

$$\frac{k(\text{SO}_4^{\bullet-}/\text{NPX})}{k(\text{SO}_4^{\bullet-}/\text{ATR})} = \frac{\ln([\text{NPX}]_0/[\text{NPX}]_t) - \ln([\text{NPX}]_0/[\text{NPX}]_t)}{\ln([\text{ATR}]_0/[\text{ATR}]_t) - \ln([\text{ATR}]_0/[\text{ATR}]_t)} \quad (5)$$

$$= \frac{k_{\text{NPX}} - k_{\text{NPX,D}}}{k_{\text{ATR}} - k_{\text{ATR,D}}}$$

Table 2
Economic comparison of removing NPX in water by three systems

Adopted process	EE/O (kWh m ⁻³ order ⁻¹)	Electricity cost ^a (\$ m ⁻³)	Oxidant costs ^b (\$ g ⁻¹)
UV alone	1.21×10^4	1.21×10^3	–
UV/PS	5.31×10^2	53.1	0.006656
UV/H ₂ O ₂	6.73×10^2	67.3	0.008439

^aElectricity cost (\$ m⁻³) = EE/O (kWh m⁻³) × 0.1 (\$ kWh⁻¹), where 0.1 (\$ kWh⁻¹) is power cost.

^bThe price of oxidant was supplied by Sinopharm Chemical Reagent Co. Ltd., Shanghai, China.

where $k(\text{SO}_4^{\bullet-}/\text{NPX})$, $k(\text{SO}_4^{\bullet-}/\text{ATR})$ represent the second-order rate constant for NPX and ATR with $\text{SO}_4^{\bullet-}$, respectively, k_{NPX} , k_{ATR} , $k_{\text{NPX,D}}$, $k_{\text{ATR,D}}$ denote the observed rate constants in UV/PS and that in the UV only, respectively. Since parts of $\text{SO}_4^{\bullet-}$ can be converted to $\bullet\text{OH}$ in the UV/PS system, TBA was used as the $\bullet\text{OH}$ quenching reagent for its reactivity with $\bullet\text{OH}$ ($k(\bullet\text{OH}/\text{TBA}) = 6.0 \times 10^8 \text{ M}^{-1} \text{ s}^{-1}$ at pH 7) which is almost three orders of magnitude higher than that with $\text{SO}_4^{\bullet-}$ ($k(\text{SO}_4^{\bullet-}/\text{TBA}) = 8.4 \times 10^5 \text{ M}^{-1} \text{ s}^{-1}$ at pH 7) [26,27]. Fig. 2 illustrates the plots of $k_{\text{NPX}} - k_{\text{NPX,D}}$ vs. $k_{\text{ATR}} - k_{\text{ATR,D}}$ for the determination of the second-order rate constants of NPX with $\text{SO}_4^{\bullet-}$ and $\bullet\text{OH}$. The plot of $k_{\text{NPX}} - k_{\text{NPX,D}}$ vs. $k_{\text{ATR}} - k_{\text{ATR,D}}$ yielded a straight line with a slope that can determine the second-order rate constants of $\text{SO}_4^{\bullet-}$ and $\bullet\text{OH}$ with NPX.

For the case of $\text{SO}_4^{\bullet-}$, the determined second-order rate constant with NPX is $7.81 \times 10^9 \text{ M}^{-1} \text{ s}^{-1}$. Similarly, the second-order rate constant between NPX and $\bullet\text{OH}$ of $6.22 \times 10^{10} \text{ M}^{-1} \text{ s}^{-1}$ was determined. It is noticeable that the second-order rate constant with $\bullet\text{OH}$ was nearly eight times higher than that with $\text{SO}_4^{\bullet-}$. However, a higher removal rate was observed during the UV/PS process than that during the UV/ H_2O_2 process (as depicted in Fig. 1). Two reasons may justify our findings. First, the production yield of $\text{SO}_4^{\bullet-}$ in the UV/PS process is higher than the production yield of $\bullet\text{OH}$ in the UV/ H_2O_2 process. This is because the radical formation quantum yield of $\text{SO}_4^{\bullet-}$ ($\epsilon = 20 \text{ M}^{-1} \text{ cm}^{-1}$ and $\Phi = 1.4$) is higher than that of $\bullet\text{OH}$ ($\epsilon = 19.6 \text{ M}^{-1} \text{ cm}^{-1}$ and $\Phi = 1.0$) [28,29]. Second, the self-scavenging of $\text{SO}_4^{\bullet-}$ by $\text{S}_2\text{O}_8^{2-}$ in the UV/PS process is greatly lower than the self-scavenging of $\bullet\text{OH}$ by H_2O_2 in the UV/ H_2O_2 process. This is also validated by the fact that the evolution of oxidant concentrations during 1 h reaction (inset of Fig. 1(a)). We can notice that the total consumption of PS was slightly higher than that of H_2O_2 under the same conditions.

3.3. Effect of oxidant concentration

The effect of oxidant concentration on the NPX degradation in the range of 0.2~8 mM ($[\text{Oxidant}]_0/[\text{NPX}]_0 = 10\sim 400$) by UV/ H_2O_2 and UV/PS processes are shown in Fig. 3.

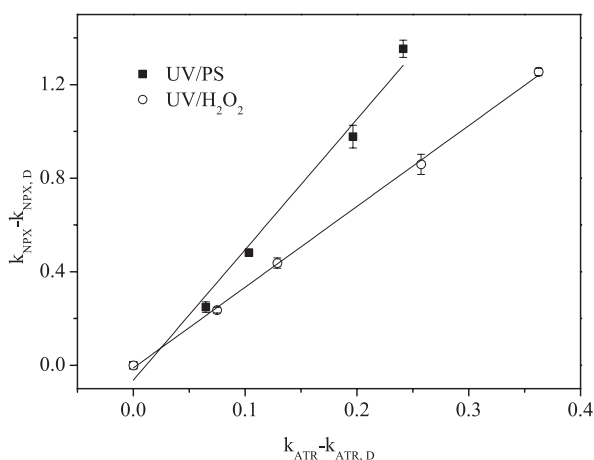


Fig. 2. Determination of the second-order rate constants of NPX with $\text{SO}_4^{\bullet-}$ and $\bullet\text{OH}$. Conditions: for $k(\text{SO}_4^{\bullet-}/\text{NPX})$ determination, $[\text{NPX}]_0 = [\text{ATR}]_0 = 20 \mu\text{M}$, $[\text{PS}]_0 = [\text{H}_2\text{O}_2]_0 = 2 \text{ mM}$, $[\text{TBA}]_0 = 100 \text{ mM}$ and pH = 7; for $k(\bullet\text{OH}/\text{NPX})$ determination, $[\text{NPX}]_0 = [\text{ATR}]_0 = 20 \mu\text{M}$, $[\text{H}_2\text{O}_2]_0 = 2 \text{ mM}$ and pH = 7.

The degradation rate constant of NPX increases from 0.0241 to 0.214 min^{-1} in the UV/PS system with the initial PS concentration increasing from 0.5 to 8 mM ($[\text{Oxidant}]_0/[\text{NPX}]_0 = 10\sim 400$). This enhancement in NPX degradation is attributable to the generation of $\text{SO}_4^{\bullet-}$ or/and $\bullet\text{OH}$ radicals as the molar ratio of PS to NPX increased. We can also observe in the inset of Fig. 3(a) that the increasing trends were linear with the initial concentration of PS ($k = 0.0263[\text{PS}]_0 + 0.01$, $R^2 = 0.99$).

In the UV/ H_2O_2 system, the degradation rate of NPX also increased from 0.0203 to 0.0913 min^{-1} , with an increase in the initial H_2O_2 concentration from 0.5 to 6 mM ($[\text{Oxidant}]_0/[\text{NPX}]_0 = 10\sim 300$). Nevertheless, unlike NPX degradation in UV/PS system, further increase in dosage has an adverse effect on the NPX degradation; the degradation rate constant of NPX decreases to 0.0854 min^{-1} when the concentration of H_2O_2 reaches 8 mM ($[\text{Oxidant}]_0/[\text{NPX}]_0 = 400$).

In the UV/ H_2O_2 system, $\bullet\text{HO}_2$ ($E_{\bullet\text{OH}_2/\text{OH}_2} = 0.79 \text{ V}$), which is less reactive than $\bullet\text{OH}$, is formed at higher H_2O_2 concentration

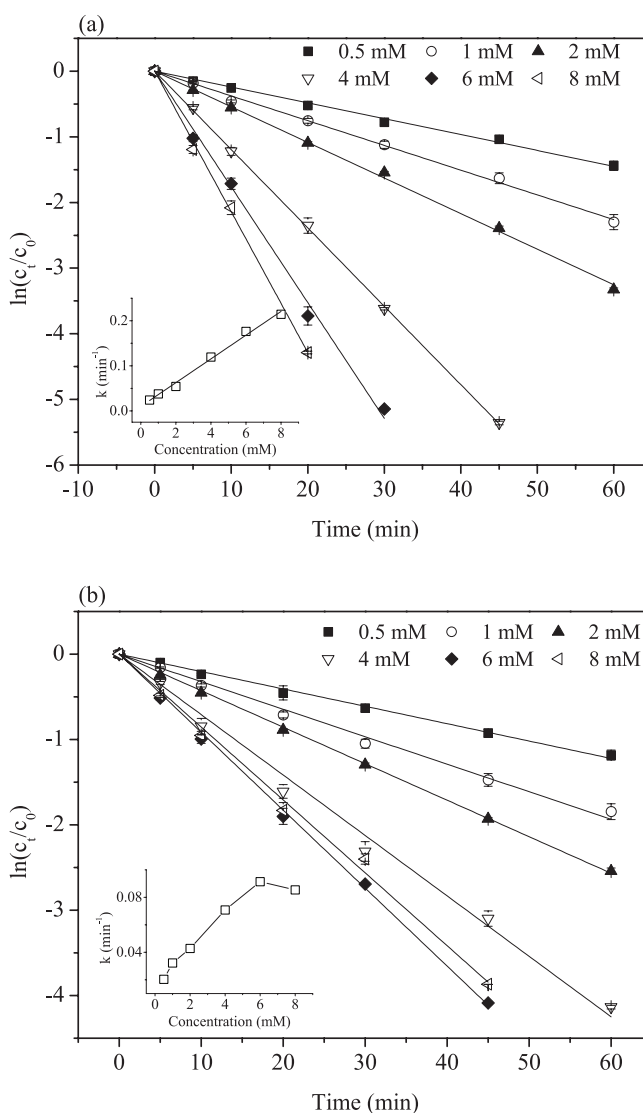
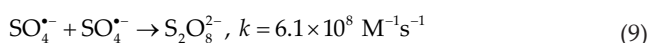
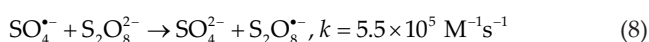
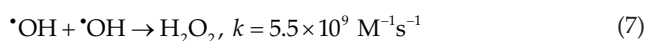
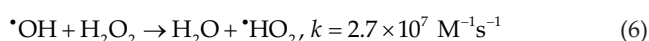


Fig. 3. Effect of oxidant concentration on NPX degradation by UV/PS and UV/ H_2O_2 . Conditions: $[\text{NPX}]_0 = 20 \mu\text{M}$, $[\text{Oxidant}]_0 = 0.2\sim 8 \text{ mM}$, pH = 7.

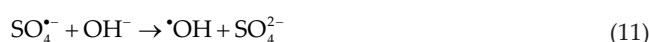
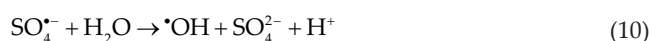
(Eq. (6)). $\bullet\text{HO}_2$ can further go through a chain termination reaction to scavenge $\bullet\text{OH}$. In addition, excess of $\bullet\text{OH}$ will dimerize to H_2O_2 according to Eq. (7); In the UV/PS system, the rate constant between $\text{SO}_4^{\bullet-}$ and $\text{S}_2\text{O}_8^{2-}$ (Eq. (8)) as well as the self-recombination rate constant of $\text{SO}_4^{\bullet-}$ was all less than in (Eq. (9)) which occurred in UV/ H_2O_2 system [27,30]. Finally, it seems that the PS concentration used here did not reach the level that started to slow down the NPX degradation:



3.4. Effect of pH

The effect of solution pH on the NPX degradation by UV/PS and UV/ H_2O_2 processes are shown in Fig. 4.

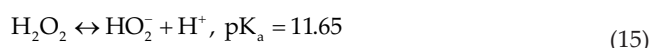
As presented in Fig. 4, the degradation rate of NPX oxidation in UV/PS and UV/ H_2O_2 processes were highly pH-dependent. In the UV/PS system, the highest degradation rate of NPX was observed at pH 3, while the rate decreased with an increase in solution pH, indicating that acidic conditions favored NPX degradation. This phenomenon can be clarified clearly. Since $\text{SO}_4^{\bullet-}$ is the dominant radical species in the acidic and neutral solutions, for negligible reaction between $\text{SO}_4^{\bullet-}$ and H_2O (Eq. (10)), and further increasing pH, $\bullet\text{OH}$ can be generated through the reaction between $\text{SO}_4^{\bullet-}$ and OH^- (Eq. (11)), and gradually playing a dominant role. As previously discussed, $\bullet\text{OH}$ displays a slower rate towards NPX degradation. Additionally, the breakdown of PS into $\text{SO}_4^{\bullet-}$ can be further acidic-catalyzed according to Eqs. (12) and (13) at pH 3 [31]. This can also favor NPX oxidation. Thus, these reasons are anticipated to obviously decrease NPX degradation efficiency under alkali conditions:



In the UV/ H_2O_2 system, the maximum degradation rate of NPX occurred at pH 6 (0.0465 min^{-1}). The degradation rate increased with pH increasing from 3 to 6, which is probably because of the scavenging effect of H^+ on $\bullet\text{OH}$ becoming less significant with the increase of the pH [32]. As derived from Nernst equation (Eq. (14)), the redox potential of $\bullet\text{OH}/\text{H}_2\text{O}$ at pH 3, 6, 7, 8 and 11 are 2.62, 2.45, 2.39, 2.33 and 2.15, respectively ($E_{\bullet\text{OH}/\text{H}_2\text{O}}^0 = 2.8 \text{ V}$). Therefore, with the increase in solution pH, the redox potential of $\bullet\text{OH}/\text{H}_2\text{O}$ is expected to also decrease, resulting in the decrease in k .

$$E_{\bullet\text{OH}} = E_{\bullet\text{OH}/\text{H}_2\text{O}}^0 - 0.059 \text{ pH} \quad (14)$$

The pK_a of H_2O_2 is 11.65, a considerable amount of H_2O_2 (approximate 18.3%), can dissociate in ionic form (Eq. (15)) at pH 11 [33]. In this case, $\bullet\text{OH}$ will be scavenged by hydroperoxide anion (HO_2^-) according to Eqs. (16) and (17) [27]. Consequently, it has been reported that the self-decomposition rate constant of H_2O_2 tended to increase with the increasing solution pH, especially at a high pH (Eq. (18)) [34]. Thus, NPX removal efficiency significantly decreased at pH 11:



3.5. Effect of chloride and bicarbonate

It is important to evaluate the effect of common anions in natural water on the degradation efficiency of NPX by UV/PS and UV/ H_2O_2 processes. This is because they have been proved to have impacts on the removal of organic contaminants through $\text{SO}_4^{\bullet-}$ and/or $\bullet\text{OH}$ -based AOPs [35]. The effects of different concentrations of chloride (Cl^-) on NPX degradation rate by UV/PS and UV/ H_2O_2 processes have been illustrated in Fig. 5(a). As observable in the Fig. 5(a), the degradation rate of NPX was enhanced under various concentrations of Cl^- in both systems. In the UV/PS system, with the concentration of Cl^- increasing to 1, 10 and 100 mM, the k increased by 8.84%, 9.20% and 19.7%, respectively. The k also increased by 7.14%, 13.20% and 14.51%, respectively, in the

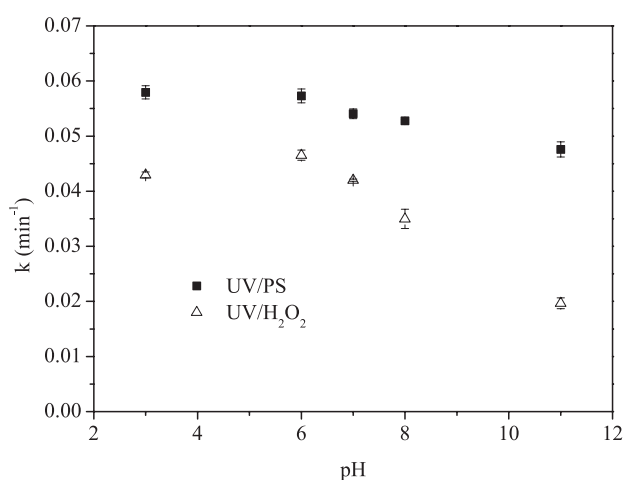
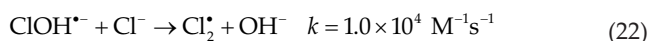
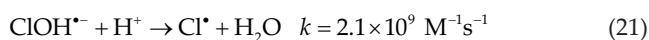
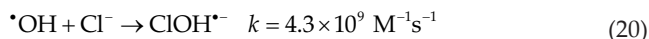
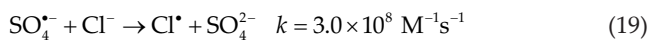


Fig. 4. Effect of solution pH on NPX degradation by UV/PS and UV/ H_2O_2 . Conditions: $[\text{NPX}]_0 = 20 \mu\text{M}$, $[\text{PS}]_0 = [\text{H}_2\text{O}_2]_0 = 2 \text{ mM}$, $\text{pH} = 3, 6, 7, 8$ and 11 .

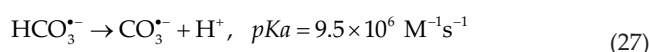
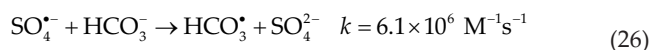
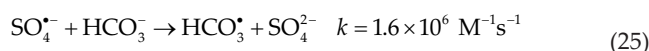
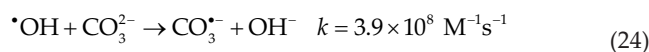
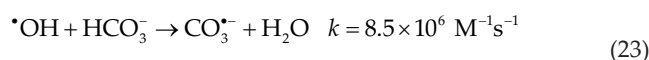
UV/H₂O₂ system. The following reactions (Eqs. (19)–(22)) that occurred in both of the systems explain our findings:



In the presence of Cl⁻, both SO₄^{•-} and •OH can react with it to generate Cl[•], ClOH^{•-} and Cl₂[•]. Among these reactive radicals, Cl[•] has a redox potential of 2.4 V. it might also participate in the NPX degradation. Therefore, except for SO₄^{•-} and •OH, Cl[•] may participate in the degradation of NPX, which can accelerate its removal. Similar results were observed by other researchers [36].

Noteworthy is that the effect of HCO₃⁻ on NPX degradation rate was opposite in two systems. The HCO₃⁻ has a

positive effect in the UV/PS system, whereas it shows a negative effect in UV/H₂O₂ system. In the presence of 1, 10 and 100 mM HCO₃⁻, the *k* improved by 3.13%, 18.49% and 13.72%, respectively in UV/PS system. However, the *k* dropped by 8.08%, 26.17% and 29.28%, respectively, in UV/H₂O₂ system. The enhancement of NPX degradation in the UV/PS system is attributable to the formation of the reactive carbonate species (CO₃^{•-}) (Eqs. (23)–(27)) [23]. The CO₃^{•-} has a positive redox potential of 1.63 V [37], which can also actively participate in the degradation of NPX. Regardless of the rates of reactions of HCO₃⁻ with SO₄^{•-} and •OH being comparable, the HCO₃⁻ is found to inhibit the NPX degradation in UV/H₂O₂ system because of the scavenging of •OH (due to their non-selective nature) by the other radical species such as HO₂[•] and O₂^{•-} present during the reaction [38].



3.6. Effect of humic acid

As illustrated in Fig. 6, the HA is found to be inhibitory to the NPX degradation in both systems, with a greater degree of inhibition in UV/H₂O₂ system than in the UV/PS system. In the UV/PS system, *k* decreased from 0.0542 to 0.0365 min⁻¹ as the HA increased from 0 to 10 mg L⁻¹. And in the UV/H₂O₂ system, *k* decreased from 0.0428 to 0.0241 min⁻¹ when the initial HA increased from 0 to 10 mg L⁻¹.

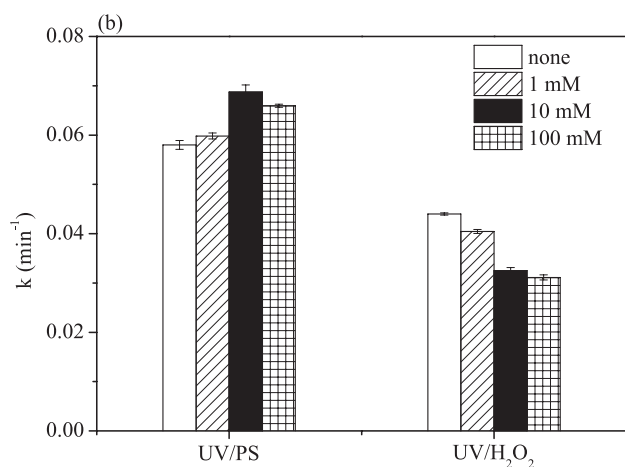
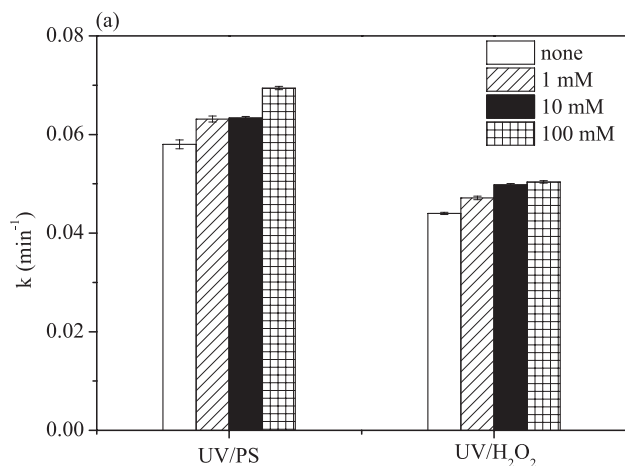


Fig. 5. Effect of (a) Cl⁻ and (b) HCO₃⁻ on NPX degradation by UV/PS and UV/H₂O₂. Conditions: [NPX]₀ = 20 μM, [PS]₀ = [H₂O₂]₀ = 2 mM, [Cl⁻]₀ = [HCO₃⁻]₀ = 1, 10 and 100 mM, no pH adjustment.

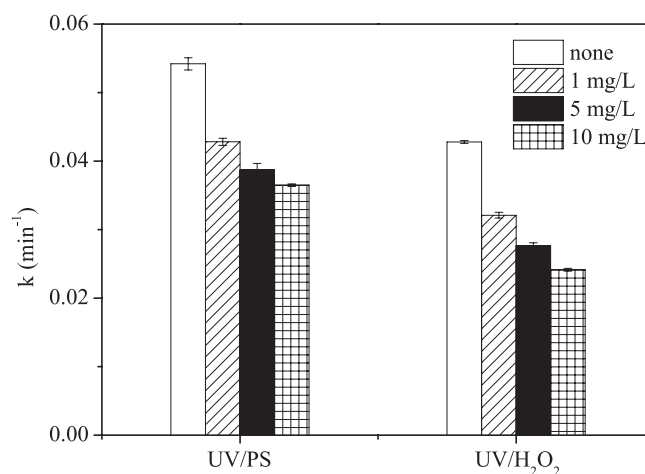


Fig. 6. Effect of HA on NPX degradation by UV/PS and UV/H₂O₂. Conditions: [NPX]₀ = 20 μM, [PS]₀ = [H₂O₂]₀ = 2 mM, [HA]₀ = 1, 5 and 10 mg L⁻¹, pH = 7.

In general, the effect of HA on targeted compounds in UV/oxidants system lies in two aspects. On the one hand, the adsorption or complexation between targeted compounds and HA promotes the compounds removal. What's more, upon adsorption of UV irradiation, the HA molecules get excited and are transformed to various reactive oxygen species that improve the degradation rate of targeted compounds [39,40]. On the other hand, the carboxyl and hydroxyl functional groups of HA can compete with targeted compounds for $\text{SO}_4^{\bullet-}$ and $\bullet\text{OH}$, which reduce the degradation efficiency of the targeted compounds [41]. Altogether, both synergistic and inhibitory effects of HA on the removal rate of target compound exist in the two systems. In addition, the stronger inhibition in the UV/ H_2O_2 system may be attributed to the scavenging of $\bullet\text{OH}$ by HA as the reported rate of reaction of HA with $\bullet\text{OH}$ being $2.23 \times 10^8 \text{ M}^{-1} \text{ s}^{-1}$ as against a lower value of 6×10^6 for $\text{SO}_4^{\bullet-}$ [38].

3.7. Degradation of NPX with natural water samples

The water quality parameters of the samples as well as the calculated pseudo-first-order rate constant are listed in Table 3. "Hengshan reservoir" and "Finished water" represent the water samples before and after treatment in one waterworks in Yixing City, Jiangsu Province, China, and "Xijiu lake" is a backup water source of the waterworks.

As displayed in Table 3, the actual water illustrated an obvious inhibition in the degradation of NPX compared with the results obtained in the deionized water. For the UV/PS process, the degradation rate was reduced by 45.4%, 36.3% and 24.7%, respectively, in three types of water compared with the deionized water. For the UV/ H_2O_2 process, the degradation rate was also reduced by 74.5%, 51.6% and 41.8%, respectively. It is evident that the organic matter has a higher impact on the degradation rate of NPX for both processes than any other water qualities. The higher the content of organic matter was, the slower the rate of NPX degradation obtained. Besides, the UV/ H_2O_2 process tend to have been more vulnerable to the constituents of the natural water due to the non-selective nature of $\bullet\text{OH}$ previously discussed.

3.8. Mineralization of NPX

Fig. 7 depicts that NPX was almost completely removed at the first 30 min during the UV/PS process and at the first 45 min in UV/ H_2O_2 process, respectively. Nonetheless, the removal rate of TOC was only 18.3% and 10.9%, respectively, even after a 2-h treatment by these two processes. We also

observed that the UV/PS process demonstrates slightly better in TOC removal in this study than the UV/ H_2O_2 process. This was consistent with its higher degradation efficiency of parent drug. The relatively low mineralization of NPX indicates that the intermediates formed during the reactions were more reluctant to the two systems as compared with its parent drug. Thus, to acquire a higher TOC elimination efficiency, the reaction conditions such as adding transition metals and increase of oxidant dosage should be carefully optimized [42,43].

4. Conclusions

In this study, we compared the degradation of NPX by the UV/PS and the UV/ H_2O_2 processes. For removal of NPX in water, the UV/PS process was realized to be superior over the direct UV irradiation or the UV/ H_2O_2 process in terms of degradation efficiency as well as cost. Higher PS dosage favored the NPX degradation, whereas an over dosage of H_2O_2 decreased NPX removal. Furthermore, NPX removal rate was decreased as the solution pH increased from 3 to 11 in the UV/PS process, whereas the optimum solution pH was 6 in the UV/ H_2O_2 process. The water matrix components also demonstrated an evident impact on the NPX degradation efficiency, which ought to be carefully considered in practical use. These results demonstrated that the UV/PS and the UV/ H_2O_2 processes are potential alternatives in the control of pollution brought about by drugs such as NPX.

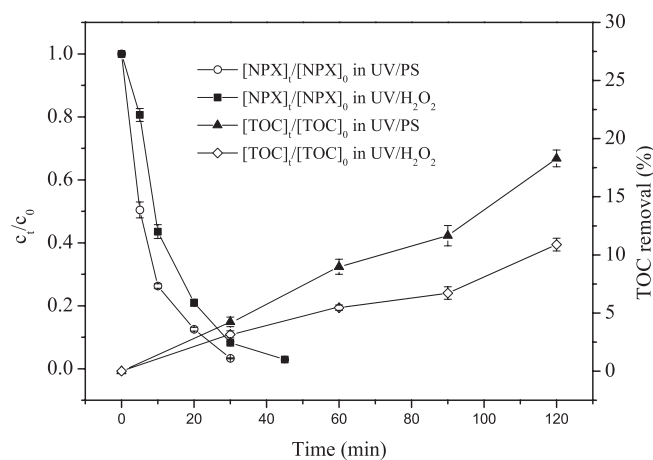


Fig. 7. The evolution of NPX concentration and TOC during the UV/PS and UV/ H_2O_2 processes. Conditions: $[\text{NPX}]_0 = 40 \mu\text{M}$, $[\text{PS}]_0 = [\text{H}_2\text{O}_2]_0 = 8 \text{ mM}$, $\text{pH} = 7$.

Table 3
Water quality parameters and pseudo-first-order rate constant of different samples^a

	pH	Cl^- (mg L^{-1})	HCO_3^- (mg L^{-1})	DOC (mg L^{-1})	k (min^{-1})	
					UV/PS	UV/ H_2O_2
Deionized water	7	0	35	0.096	0.0542	0.0428
Xijiu lake	7.86	24	146	15.66	0.0296	0.0109
Hengshan reservoir	7.63	6	126	5.919	0.0345	0.0207
Finished water	7.70	14	134	4.092	0.0408	0.0249

^a $[\text{NPX}]_0 = 20 \mu\text{M}$, $[\text{PS}]_0 = [\text{H}_2\text{O}_2]_0 = 2 \text{ mM}$, reaction time = 1 h.

Acknowledgments

This work was supported by the Foundation of Key Laboratory of Yangtze River Water Environment, Ministry of Education, Tongji University, China (YRWEF201601) and the national major project of Science and Technology Ministry of China (No. 2012ZX07403-001). The authors are also thankful to the reviewers and editors for their valuable advice to improve the manuscript.

References

- [1] P. Grenni, L. Patrolecco, N. Ademollo, A. Tolomei, A.B. Caracciolo, Degradation of gemfibrozil and naproxen in a river water ecosystem, *Microchem. J.*, 107 (2013) 158–164.
- [2] M. Carballa, F. Omil, J.M. Lema, M. Llompert, C. García-Jares, I. Rodríguez, M. Gómez, T. Ternes, Behavior of pharmaceuticals, cosmetics and hormones in a sewage treatment plant, *Water Res.*, 38 (2004) 2918–2926.
- [3] T.A. Ternes, Occurrence of drugs in German sewage treatment plants and rivers, *Water Res.*, 32 (1998) 3245–3260.
- [4] L.H. Santos, A.N. Araújo, A. Fachini, A. Pena, C. Delerue-Matos, M. Montenegro, Ecotoxicological aspects related to the presence of pharmaceuticals in the aquatic environment, *J. Hazard. Mater.*, 175 (2010) 45–95.
- [5] J.L. Zhou, Z.L. Zhang, E. Banks, D. Grover, J.Q. Jiang, Pharmaceutical residues in wastewater treatment works effluents and their impact on receiving river water, *J. Hazard. Mater.*, 166 (2009) 655–661.
- [6] M. Isidori, M. Lavorgna, A. Nardelli, A. Parrella, L. Previtiera, M. Rubino, Ecotoxicity of naproxen and its phototransformation products, *Sci. Total Environ.*, 348 (2005) 93–101.
- [7] M. Manrique-Moreno, M. Suwalsky, F. Villena, P. Garidel, Effects of the nonsteroidal anti-inflammatory drug naproxen on human erythrocytes and on cell membrane molecular models, *Biophys. Chem.*, 147 (2010) 53–58.
- [8] S. Canonica, L. Meunier, U. von Gunten, Phototransformation of selected pharmaceuticals during UV treatment of drinking water, *Water Res.*, 42 (2008) 121–128.
- [9] V.J. Pereira, H.S. Weinberg, K.G. Linden, P.C. Singer, UV degradation kinetics and modeling of pharmaceutical compounds in laboratory grade and surface water via direct and indirect photolysis at 254 nm, *Environ. Sci. Technol.*, 41 (2007) 1682–1688.
- [10] P. Avetta, A. Pensato, M. Minella, M. Malandrino, V. Maurino, C. Minero, K. Hanna, D. Vione, Activation of persulfate by irradiated magnetite: implications for the degradation of phenol under heterogeneous photo-fenton like conditions, *Environ. Sci. Technol.*, 49 (2015) 1043–1050.
- [11] C.S. Liu, K. Shih, C.X. Sun, F. Wang, Oxidative degradation of propachlor by ferrous and copper ion activated persulfate, *Sci. Total Environ.*, 416 (2012) 507–512.
- [12] Y.Q. Gao, N.Y. Gao, Y. Deng, Y.Q. Yang, Y. Ma, Ultraviolet (UV) light-activated persulfate oxidation of sulfamethazine in water, *Chem. Eng. J.*, 195 (2012) 248–253.
- [13] Y.Q. Gao, N.Y. Gao, Y. Deng, D.Q. Yin, Y.S. Zhang, W.L. Rong, S.D. Zhou, Heat-activated persulfate oxidation of sulfamethoxazole in water, *Desal. Wat. Treat.*, 56 (2015) 2225–2233.
- [14] Q. Yang, H. Choi, Y.J. Chen, D.D. Dionysiou, Heterogeneous activation of peroxymonosulfate by supported cobalt catalysts for the degradation of 2,4-dichlorophenol in water: the effect of support cobalt precursor and UV radiation, *Appl. Catal., B*, 77 (2008) 300–307.
- [15] S. Zorita, L. Mårtensson, L. Mathiasson, Occurrence and removal of pharmaceuticals in a municipal sewage treatment system in the south of Sweden, *Sci. Total Environ.*, 407 (2009) 2760–2770.
- [16] W.H. Chu, T.F. Chu, E.D. Du, Y. Deng, Y.Q. Guo, N.Y. Gao, Increased formation of halomethanes during chlorination of chloramphenicol in drinking water by UV irradiation, persulfate oxidation, and combined UV/persulfate pretreatments, *Ecotoxicol. Environ. Saf.*, 124 (2016) 147–154.
- [17] F.J. Beltrán, G. Ovejero, J.F. Garcia-Araya, J. Rivas, Oxidation of polynuclear aromatic hydrocarbons in water. 2. UV radiation and ozonation in the presence of UV radiation, *Ind. Eng. Chem. Res.*, 34 (1995) 1607–1615.
- [18] C.J. Liang, C.F. Huang, N. Mohanty, R.M. Kurakalva, A rapid spectrophotometric determination of persulfate anion in ISCO, *Chemosphere*, 73 (2008) 1540–1543.
- [19] J. De Laat, H. Gallard, Catalytic decomposition of hydrogen peroxide by Fe (III) in homogeneous aqueous solution: mechanism and kinetic modeling, *Environ. Sci. Technol.*, 33 (1999) 2726–2732.
- [20] J.R. Bolton, M.I. Stefan, Fundamental photochemical approach to the concepts of fluence (UV dose) and electrical energy efficiency in photochemical degradation reactions, *Res. Chem. Intermed.*, 28 (2002) 857–870.
- [21] A. Lopez, A. Bozzi, G. Mascolo, J. Kiwi, Kinetic investigation on UV and UV/H₂O₂ degradations of pharmaceutical intermediates in aqueous solution, *J. Photochem. Photobiol. A*, 156 (2003) 121–126.
- [22] V.J. Pereira, K.G. Linden, H.S. Weinberg, Evaluation of UV irradiation for photolytic and oxidative degradation of pharmaceutical compounds in water, *Water Res.*, 41 (2007) 4413–4423.
- [23] Y.Q. Liu, X.X. He, Y.S. Fu, D.D. Dionysiou, Kinetics and mechanism investigation on the destruction of oxytetracycline by UV-254 nm activation of persulfate, *J. Hazard. Mater.*, 305 (2016) 229–239.
- [24] F.J. Beltrán, G. Ovejero, B. Acedo, Oxidation of atrazine in water by ultraviolet radiation combined with hydrogen peroxide, *Water Res.*, 27 (1993) 1013–1021.
- [25] M.E.D.G. Azenha, H.D. Burrows, M. Canle L., R. Coimbra, M.I. Fernández, M.V. García, M.A. Peiteado, J.A. Santaballa, Kinetic and mechanistic aspects of the direct photodegradation of atrazine, atraton, ametryn and 2-hydroxyatrazine by 254 nm light in aqueous solution, *J. Phys. Org. Chem.*, 16 (2003) 498–503.
- [26] R.E. Huie, C.L. Clifton, Rate constants for hydrogen abstraction reactions of the sulfate radical, SO₄^{•-}, *Alcohols*, *Int. J. Chem. Kinet.*, 21 (1989) 611–619.
- [27] G.V. Buxton, C.L. Greenstock, W.P. Helman, A.B. Ross, Critical review of rate constants for reactions of hydrated electrons, hydrogen atoms and hydroxyl radicals (•OH/•O⁻) in aqueous solution, *J. Phys. Chem. Ref. Data*, 17 (1988) 513–886.
- [28] J.H. Baxendale, J.A. Wilson, The photolysis of hydrogen peroxide at high light intensities, *Trans. Faraday Soc.*, 53 (1957) 344–356.
- [29] G. Mark, M.N. Schuchmann, H.P. Schuchmann, C. von Sonntag, The photolysis of potassium peroxodisulphate in aqueous solution in the presence of tert-butanol: a simple actinometer for 254 nm radiation, *J. Photochem. Photobiol. A*, 55 (1990) 157–168.
- [30] X.Y. Yu, Z.C. Bao, J.R. Barker, Free radical reactions involving Cl[•], Cl₂^{•-}, and SO₄^{•-} in the 248 nm photolysis of aqueous solutions containing S₂O₈²⁻ and Cl⁻, *J. Phys. Chem. A*, 108 (2004) 295–308.
- [31] C.J. Liang, Z.S. Wang, C.J. Bruell, Influence of pH on persulfate oxidation of TCE at ambient temperatures, *Chemosphere*, 66 (2007) 106–113.
- [32] C.Q. Tan, N.Y. Gao, Y. Deng, Y.J. Zhang, M.H. Sui, J. Deng, S.Q. Zhou, Degradation of antipyrine by UV, UV/H₂O₂, and UV/PS, *J. Hazard. Mater.*, 260 (2013) 1008–1016.
- [33] D.A. Vander Griend, J.S. Golden, C.A. Arrington, Jr., Kinetics and mechanism of chromate reduction with hydrogen peroxide in base, *Inorg. Chem.*, 41 (2002) 7042–7048.
- [34] W. Chu, Modeling the quantum yields of herbicide 2,4-D decay in UV/H₂O₂ process, *Chemosphere*, 44 (2001) 935–941.
- [35] Y. Yang, J.J. Pignatello, J. Ma, W.A. Mitch, Comparison of halide impacts on the efficiency of contaminant degradation by sulfate and hydroxyl radical-based advanced oxidation processes (AOPs), *Environ. Sci. Technol.*, 48 (2014) 2344–2351.
- [36] Q.F. Wang, Y.S. Shao, N.Y. Gao, W.H. Chu, S. Xiang, X. Lu, J.X. Chen, Y.P. Zhu, Degradation kinetics and mechanism of 2,4-Di-tert-butylphenol with UV/persulfate, *Chem. Eng. J.*, 304 (2016) 201–208.

- [37] Z.H. Zuo, Z.L. Cai, Y. Katsumura, N. Chitose, Y. Muroya, Reinvestigation of the acid-base equilibrium of the (bi)carbonate radical and pH dependence of its reactivity with inorganic reactants, *Radiat. Phys. Chem.*, 55 (1999) 15–23.
- [38] J. Sharma, I.M. Mishra, V. Kumar, Degradation and mineralization of bisphenol A (BPA) in aqueous solution using advanced oxidation processes: UV/H₂O₂ and UV/S₂O₈²⁻ oxidation systems, *J. Environ. Manage.*, 156 (2015) 266–275.
- [39] B. Roshani, N.K.V. Leitner, The influence of persulfate addition for the degradation of micropollutants by ionizing radiation, *Chem. Eng. J.*, 168 (2011) 784–789.
- [40] J. Wenk, U. von Gunten, S. Canonica, Effect of dissolved organic matter on the transformation of contaminants induced by excited triplet states and the hydroxyl radical, *Environ. Sci. Technol.*, 45 (2011) 1334–1340.
- [41] X.G. Gu, S.G. Lu, Z.F. Qiu, Q. Sui, Z.W. Miao, K.F. Lin, Y.D. Liu, Q.S. Luo, Comparison of photodegradation performance of 1,1,1-trichloroethane in aqueous solution with the addition of H₂O₂ or S₂O₈²⁻ oxidants, *Ind. Eng. Chem. Res.*, 51 (2012) 7196–7204.
- [42] J. Criquet, N.K.V. Leitner, Degradation of acetic acid with sulfate radical generated by persulfate ions photolysis, *Chemosphere*, 77 (2009) 194–200.
- [43] J.A. Khan, X.X. He, H.M. Khan, N.S. Shah, D.D. Dionysiou, Oxidative degradation of atrazine in aqueous solution by UV/H₂O₂/Fe²⁺, UV/S₂O₈²⁻/Fe²⁺ and UV/HSO₅⁻/Fe²⁺ processes: a comparative study, *Chem. Eng. J.*, 218 (2013) 376–383.